LBL-21354
c.2

RECEIVED
LAWRENCE
BERKELEY LABORATOR

AUG 12 1986

LIBRARY AND
DOCUMENTS SECTIO

LBL-21354

Presented at the
'86 International Conference on
Trends in Welding Research,
Gatlinburg, TN, May 19-22, 1986

MICROSTRUCTURAL REFINEMENT THROUGH MULTIPASS GTAW PROCESS

H.-J. Kim and J.W. Morris, Jr.

April 1986

TWO-WEEK LOAN COPY

This is a Library Circulating Copy which may be borrowed for two weeks.

Lawrence Berkeley Laboratory
University of California
Berkeley, California 94720

Prepared for the U.S. Department of Energy
under Contract DE-AC03-76SF00098

Center for Advanced Materials

LBL-21354
c.2

DISCLAIMER

This document was prepared as an account of work sponsored by the United States Government. While this document is believed to contain correct information, neither the United States Government nor any agency thereof, nor the Regents of the University of California, nor any of their employees, makes any warranty, express or implied, or assumes any legal responsibility for the accuracy, completeness, or usefulness of any information, apparatus, product, or process disclosed, or represents that its use would not infringe privately owned rights. Reference herein to any specific commercial product, process, or service by its trade name, trademark, manufacturer, or otherwise, does not necessarily constitute or imply its endorsement, recommendation, or favoring by the United States Government or any agency thereof, or the Regents of the University of California. The views and opinions of authors expressed herein do not necessarily state or reflect those of the United States Government or any agency thereof or the Regents of the University of California.

MICROSTRUCTURAL REFINEMENT THROUGH MULTIPASS GTAW PROCESSS

Hee-Jin Kim and J.W. Morris, Jr.

Lawrence Berkeley Laboratory
University of California
Berkeley, California 94720

April 1986

MICROSTRUCTURAL REFINEMENT THROUGH MULTIPASS GTAW PROCESS

Hee-Jin Kim and J.W. Morris, Jr.

ABSTRACT

The present work was undertaken to illustrate and clarify the microstructural features of martensitic Fe-Ni weld deposits made by a multipass welding process. To simulate this, rapid thermal treatments were applied to an Fe-12Ni-0.25Ti alloy using (1) an induction furnace and (2) bead-on-plate welding. The rapid thermal treatment refines the microstructure significantly by destroying the previous packet structure. Hence, the term "packet refinement" is used to distinguish its microstructural features from the grain refinement associated with recrystallization of austenite. During multipass GTAW process with an 11% Ni ferritic filler wire, a coarse columnar grain structure is formed after solidification but this structure is refined repetitively by the rapid thermal cycles of subsequent passes. The result is a fully packet refined and extremely fine structure, in the order of several microns, throughout the weldment.

THE THERMAL HISTORY of a weld thermal cycle is highly dynamic. Hence, the solid-solid phase transformations experienced in a welded region are different from those during conventional furnace or thermomechanical heat treatment. The weld cycle accomplishes either a very rapid austenitizing cycle or a very short time tempering treatment depending on its peak temperatures. Previously, the present authors [1,2] applied rapid thermal cycles to 9 and 12% Ni steels to simulate the microstructural changes occurring in the HAZ. These studies demonstrated that the simulated HAZ microstructures are quite different from those obtained by corresponding furnace heat treatments. For instance, a rapid austenitizing cycle refines the microstructure by destroying the previous packet structure (packet refinement) while an austenitizing treatment performed in the furnace for a longer time refines the size of the prior austenite grains (grain refinement) through the recrystallization process. It was also demonstrated that the multi-cycle treatment was more effective in refining the effective grain size and, thus, suppressed the ductile-brittle transition temperature (DBTT). The present research was performed to extend these microstructural studies to actual multipass weld deposits. The first part of the paper will described the effect of simulated weld thermal cycles in an induction furnace. The microstructural features obtained after this treatment have been published elsewhere [2] but some of them are quoted here to help in the understanding of the characterisitcs of "packet refinement". Later, the microstructural changes due to actual weld thermal cycles applied in the HAZ of bead-on-plate weldment and in the multipass weld deposit are presented. In the multipass weldment, each bead is expected to experience weld thermal cycles due to subsequent passes and is thus packet-refined repetitively to yield a very fine structure.

MATERIALS AND EXPERIMENTAL PROCEDURE

RAPID THERMAL CYCLES - The alloy used for cyclic treatment has the nominal composition of Fe-12Ni-0.25Ti with less than 0.01C. A plate of this alloy was annealed at 1200C for three hours furnace cooled to 900C and quenched in water. Its condition is designated as 'AN'. The 'AN' plate was machined and sliced to slightly oversized Charpy specimens. Single and double austenitizing cycles were applied to these specimens in an induction furnace. During this treatment, the specimen was heated to 790C within 15 seconds and then immediately dropped into an oil bath. A single such cycle constitutes the 'C' treatment: a double cycle is designated 'CC'.

BEAD-ON-PLATE WELDMENT - In order to investigate the effect of peak temperature on microstructure, a GTAW bead-on-plate weld was made on the annealed Fe-12Ni-0.25Ti alloy (AN). Its HAZ microstructure was analyzed by both optical and fractographic means. To perform the fractographic analysis, the welded plates were sliced into standard Charpy specimens and then temper embrittled at 450C for 500 hours. After inserting a 0.2 mm saw cut within the weld metal as shown in Fig. 1, the embrittled specimens were hydrogen charged in a solution of 1 N sulfuric acid at a current density of 10 mA/mmA. The hydrogen-charged specimens were bolt loaded immediately after charging to initiate and to propagate a crack through the HAZ. After the crack ceased propagating into the base metal, the half broken specimens were fractured into two pieces. This method is quite effective in promoting intergranular fracture in the annealed or the recrystallized specimens [2]. The fractographic information obtained was correlated with the corresponding microstructure revealed on the etched specimen.

MULTIPASS GTAW WELDMENT - A fully weld deposit material was fabricated by building up weld beads on the 24.5 mm thick 9% Ni steel plate. Using a fully automated GTAW process, weld beads were deposited side by side and layer by layer until the size of the weld deposit reached about 11 x 38 x 3.6 cm. The chemical compositon of the filler wire and weld deposit are shown in Table 1. The weld deposit contains 11% Ni and a very low content of interstitial elements.

Weld deposit samples for optical microscopy were polished and etched with a 5% Nital or an acidified ferric chloride solution. Samples for transmission electron microscopy were spark-cut from chemically-thinned slices of weld deposit. They were electropolished in a twin jet polishing apparatus using a chromic-acetic acid solution. The specimens were examined in a Philips 301 electron microscopy at 100 kV.

RESULTS

MICROSTRUCTURE OF THE THERMALLY CYCLED SPECIMENS - The microstructure of the 12Ni alloy in the annealed and quenched (AN) state is illustrated by the optical micrograph in Fig. 2a. This micrograph shows coarse grains of the prior austenite phase, each of which is subdivided into several packets of lath martensite. The boundaries of the packets are irregular, as evidenced by their jagged appearance in the plane of the micrograph and by the appearance of islands of one packet in the interior of its neighbor. Detailed TEM studies performed on this micro-

structure [2] showed that a single martensite variant is present within a packet. The packet size is the effective grain size governing transgranular cleavage since each packet shares a (100) cleavage plane. The microstructure of the alloy in single and double, cycled conditions ('C' and 'CC', respectively) are shown in Figs. 2b and 2c. In the 'C' condition the prior austenite grain boundaries are roughened and partly obscured by the martensite transformation products formed across the boundaries. In 'CC' condition prior austenite grain boundaries can hardly be found and the original packet structure was completely and homogeneously destroyed into very fine scale. There is no evidence of recrystallization, i.e., nucleation of new austenite grains and growth in the 'C' and 'CC' microstructures. Following the fractographic and TEM evidence, the present authors [2] have used the term 'packet refinement' to distinguish this kind of microstructural change from the 'grain refinement' associated with the conventional austenitizing treatment.

HAZ MICROSTRUCTURE OF THE BEAD-ON-PLATE WELDMENT - The bead-on-plate welding process generates high rates of heating and cooling in the parent metal adjacent to the weld and produces a band of HAZ surrounding the fused weld metal. The HAZ extends from the fusion line, which experiences the liquidus temperature, to an outer location heated to a lower critical temperature. By investigating the HAZ microstructure from fusion line to outer limit, the microstructural changes due to successively lower peak temperatures can be assessed. The macroscopic view of a bead-on-plate weld made on an annealed 12Ni plate is shown in Fig. 3. As can be seen in this figure, the HAZ structure, which extends about 5mm from the fusion line, has a much finer grain structure than the base metal. This feature becomes more clear in the magnified picture (Fig. 4) taken across the HAZ. To visualize the small grains formed along the fusion boundary, fractographic analysis was performed using the method described earlier. The result is represented in the SEM fractographs shown in Fig. 5. As shown in Fig. 5a, the columnar grains in the weld metal and the equiaxed grains in the HAZ immediately adjacent to the fusion line fracture in an intergranular mode. However, the fracture mode suddenly changes to ductile dimple in the outer side of HAZ and then to intergranular again in the base metal. Figure 4b clearly illustrates the equiaxed HAZ grains next to the fusion boundary, as well as the columnar grains grown on the half-melted HAZ grains. These grains are much smaller than the base metal grains as observed in the optical means. It follows that grain refinement took place in the area surrounding the weld metal to a width of about 100 `m during the weld thermal cycle. It is also clear from Fig. 4 that the grains become smaller with increasing distance from the fusion line, i.e., with lowering of peak temperature.

In contrast to the grain refinment near the fusion boundary, the microstructural refinement in the outer region of HAZ seems to be accomplished by the destruction of the original packet structure, i.e., by 'packet refinement' [2]. The packet refinement is illustrated in the bottom of Fig. 4. In the boundary area between the HAZ and the base metal, a portion of the base metal grain is destroyed but the other half of the grain preserves its original shape. In the packet-refined region, the microstructure is quite similar to that in the 'C' specimen (Fig. 2b). Optical examination of the cross-section of the broken specimen shows that the ductile dimple region of the fracture surface

shown in Fig. 5a matches well with the packet-refined part of the HAZ. Figure 6 shows partially overlapped bead-on-plate weldments. Detailed examination of the weld metal structure shows the elongated columnar grains of the previous equiaxed grains next to the fusion line and the 'packet-refined' structure in the outer HAZ. The columnar grains formed in earlier passes did not coarsen but were mostly refined into fine grains or packets during the weld thermal cycle of subsequent passes.

MICROSTRUCTURE OF MULTIPASS WELD DEPOSIT - As described in section II, an all-weld deposit plate was fabricated and its microstructure studied with optical and transmission electron microscopy. The characterization specimens were sliced perpendicular to the welding direction. Figures 7a and 7b show optical microstructures after etching with 5% Nital and acidified $FeCl_3$ solutions, respectively. Figure 7a shows the cellular solidification structure that is typical in the Fe-(9-12)Ni system [3,4]. Even though the solidification structure is preserved, the transformed structure of the weld deposit is severely packet refined, as shown in Figure 7b. The microstructure is quite similar to that of double-cycled specimen ('CC') shown in Fig. 2c. The results of transmission electron microscope (TEM) are presented in Fig. 8. The area shown in the bright field micrograph contains at least three different orientations that yield distinct martensite diffraction patterns as shown in the figure. The distinct variants can be separated with dark field techniques as shown in Figures 8c, d and e. The boundaries between areas having different orientations are jagged and have sharp edges indicating that they are more like packet boundaries than grain boundaries. No grain boundary-like feature, i.e., smooth boundaries, was observed throughout the TEM examination. The TEM study demonstrates that different martensite variants are intermixed on a very fine scale resulting in an extremely fine effective grain size, in the order of several microns.

DISCUSSION

It is clear from the above that the HAZ in Fe-9-12Ni steels contains two regions with distinctly different microstructures: (a) a grain-refined region and (b) a 'packet-refined' region. The grain-refined region borders the weld metal while the packet-refined region constitutes most of HAZ. The results indicate that the type of refinement depends on the peak temperature of the weld thermal cycle. Immediately adjacent to the fusion boundary, the parent metal is raised to a temperature well above the austenite transformation temperature. Substantially complete transformation to austenite takes place, and the temperature is high enough for nucleation and growth of new austenite grains to occur. Maki [5] and others [6] have proposed that the driving force for recrystallization is the strain energy in the austenite phase after reverse shear transformation. If the recrystallized grains are smaller (or larger) than the original grains, the term 'grain refined (or coarsened) region' can be used to describe the resulting microstructure. Further away from the fusion boundary, the peak temperature is lower. Where the transformation temperature is exceeded but the recrystallization temperature (or time) is not, the austenite formed by the reverse shear transformation has a high residual defect density. Given the high density of defects and the propensity for the heterogeneous nucleation of martensite on cooling, it appears that the cooperative

growth of adjacent laths is suppressed so that martensite laths from in small elements whose variants are more randomly chosen from among the 24 variants permitted by the Kurdjumov-Sachs (K-S) orientation relationship. This results in the destruction of the previous packet and in the 'packet-refined' structure.

In the case of a multipass weldment the as-cast columnar grains can be grain-refined and/or packet refined by subsequent passes. Moreover, if the HAZ of successive packets overlaps, the refined structures are further refined into fine packet structures by the rapid thermal cycles associated peak with still latter passes. This results in a fully refined packet and extremely fine structure throughout the weldment (effective grain site of several microns), as shown in Figs. 7 and 8. The fine effective grain size and the absence of clear prior austenite boundaries suggest that the multipass weld deposit may have exceptional resistance to low temperature cleavage and to embrittlement by tempering or hydrogen. The result of appropriate tests will be presented separately.

CONCLUSION

The microstructural refinement in the HAZ of weldments in 9-12Ni steel consists of grain refinment near the fusion boundary and packet refinement in the bulk of the HAZ. In the case of multipass weldment, the fine grains formed near the fusion boundary are further refined into fine packets by the weld thermal cycles of subsequent passes to lower peak temperatures. If the successive packets overlap, this results in a wholly packet refined structure.

ACKNOWLEDGEMENTS

This work was supported by the Director, Office of Energy Research, Office of Basic Energy Science, Material Science Division of the U.S. Department of Energy under contract No. DE-AC03-76SF00098.

REFERENCES

1. Kim, H.J., H. Shin and J.W. Morris, Jr., Proc. of Int. Cryo. Mat. Conf., Kobe, Japan, pp. 129-133 (1982)
2. Kim, H.J., Y.H. Kim and J.W. Morris, Jr., Lawrence Berkeley Laboratory Report #17617, Berkeley, CA 94720 (1982)
3. Devletion, J.H., J.R. Stephen and W.R. Witzke, Welding J., 56:4, 97-102S (1977)
4. Agusa, K., M. Koshio, N. Nishiyama, A. Kamada and Y. Nakano, Kawasaki Steel Technical Report No. 6, pp. 1-11 (1982)
5. Maki, T., H. Morimoto and I. Tamura, Trans. ISIJ, 20:10, pp. 700-706 (1980)
6. Nakazawa, K., Y. Kawabe and S. Muneki, Trans. ISIJ, 23:4, pp. 347-356 (1983)

Table 1. Chemical Composition of Filler and Weld Material.

Material	C	Ni	Mn	Si	P	S	Fe
Filler Wire	0.01	11.0	0.39	0.02	0.003	0.002	bal.
Weld Metal	0.01	11.0	0.39	0.02	-	-	bal.

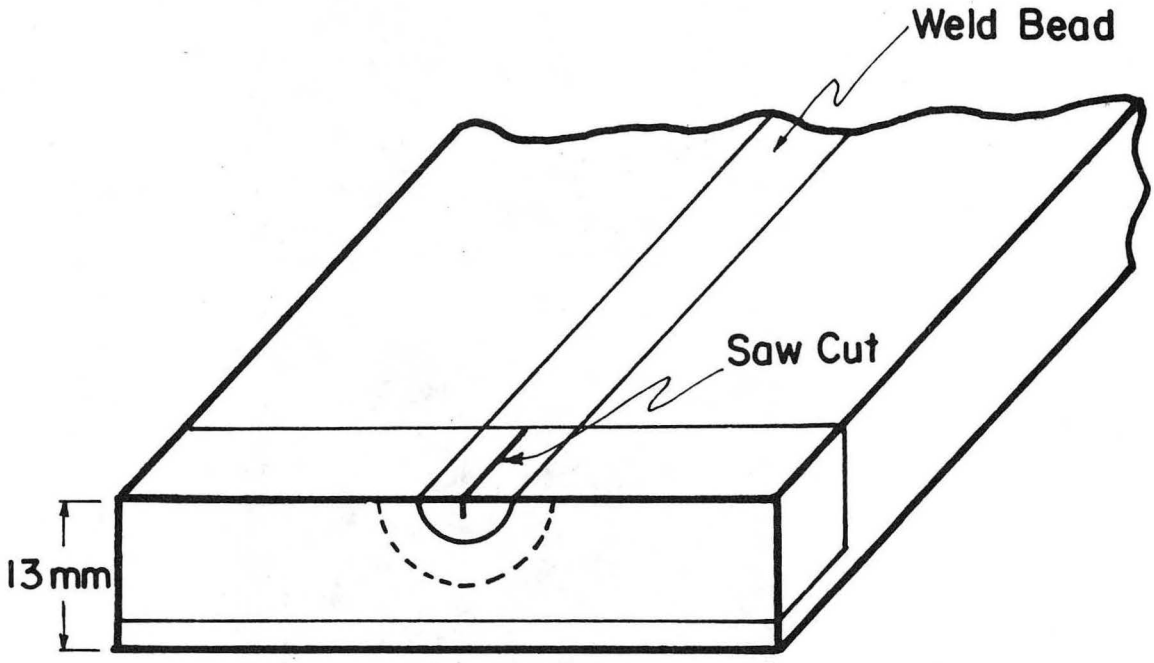

XBL847-7186

Fig. 1 - Schematical drawing of bead-on-plate weldment and location of specimens taken for the fractographic analysis.

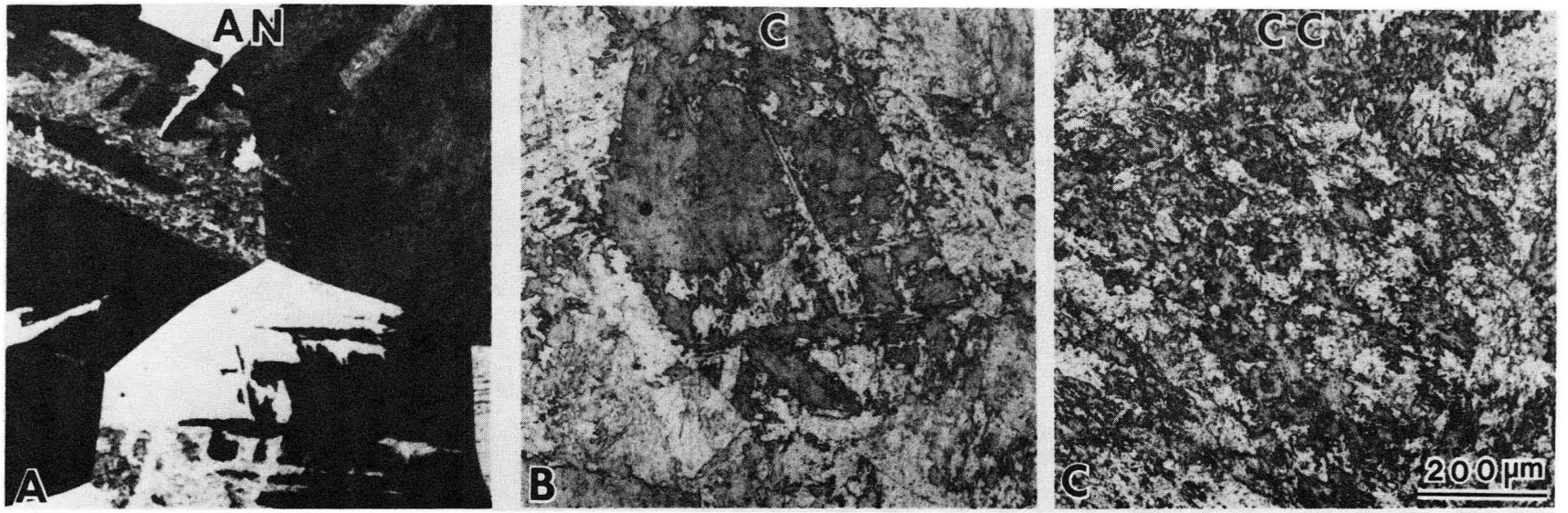

XBB 855-4037

Fig. 2 - Optical micrographs of 12Ni alloy: (a) anneal and quenched (AN), (b) a single cycled, and (c) double-cycled conditions.

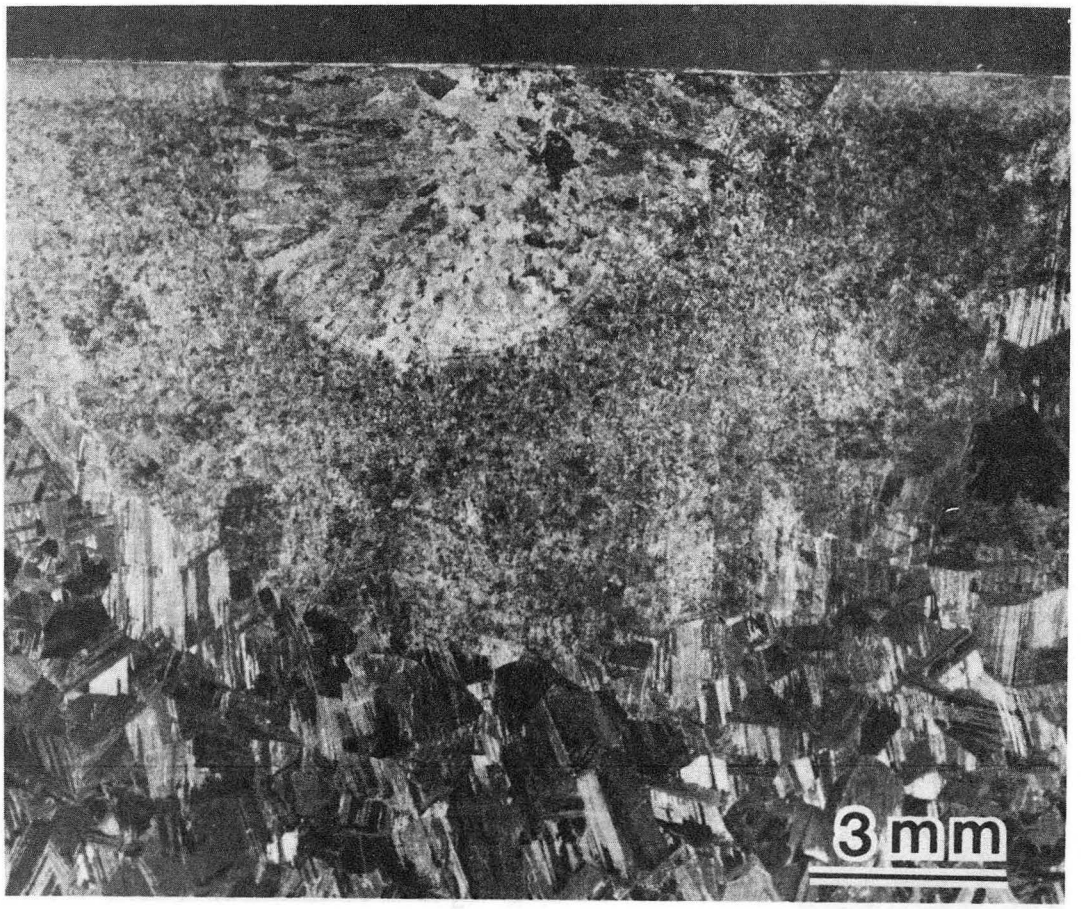

XBB 843-2117

Fig. 3 - Microstructure of the bead-on-plate weldment.

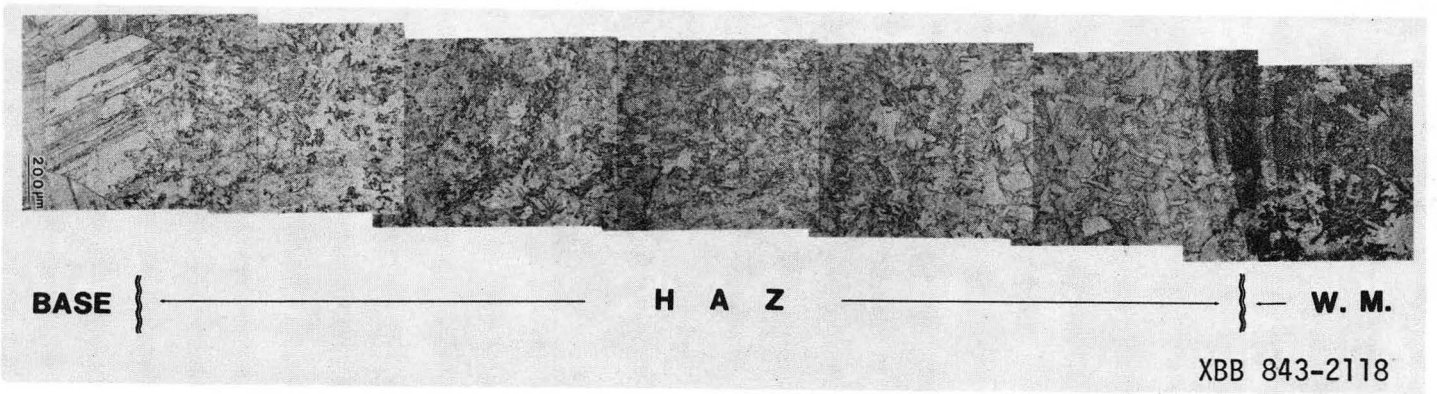

Fig. 4 - Optical picture of bead-on-plate weldment showing the distinguishable change in microstructure across the HAZ.

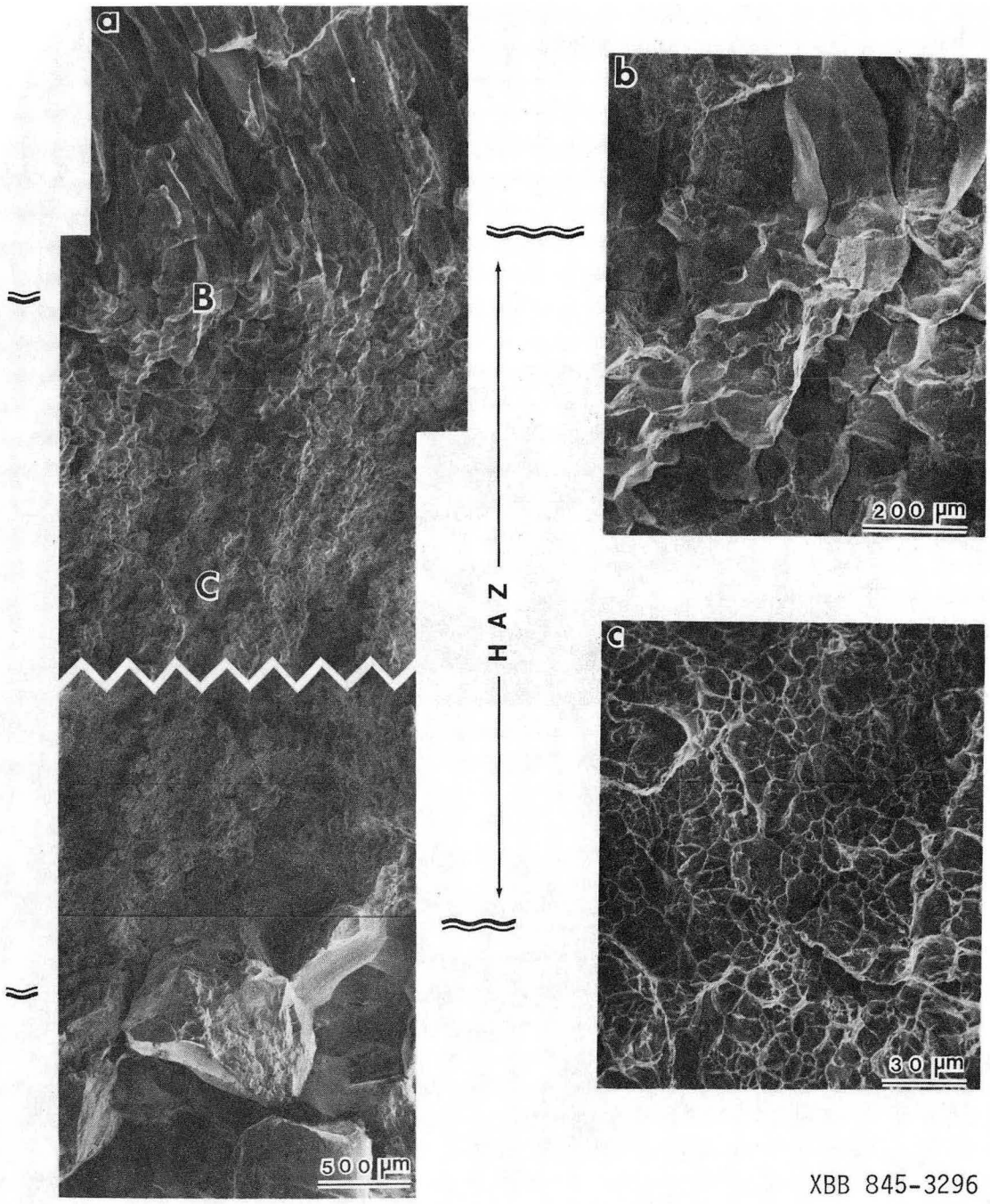

XBB 845-3296

Fig. 5 - SEM fractographs showing (a) the fracture mode change occurring from weld metal to base metal, (b) and (c) are the magnification of the areas maked B and C, respectively in (a).

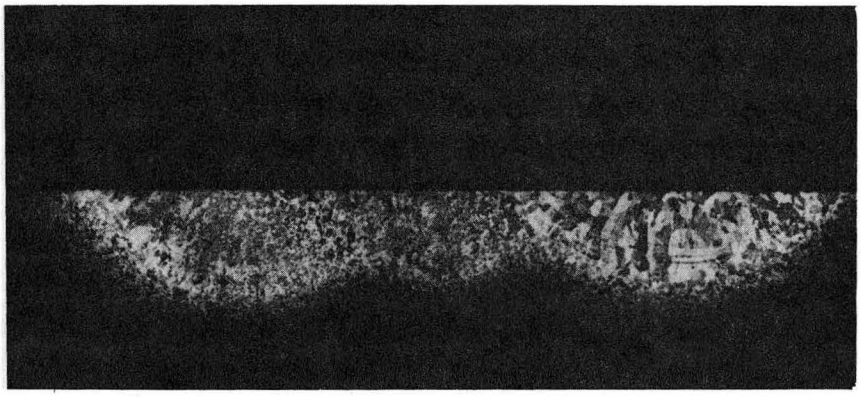

XBB 805-6225A

Fig. 6 - Microstructure of all weld deposit speciman etched with (a) 5% Nital and (b) acidified $FeCl_3$ solutions.

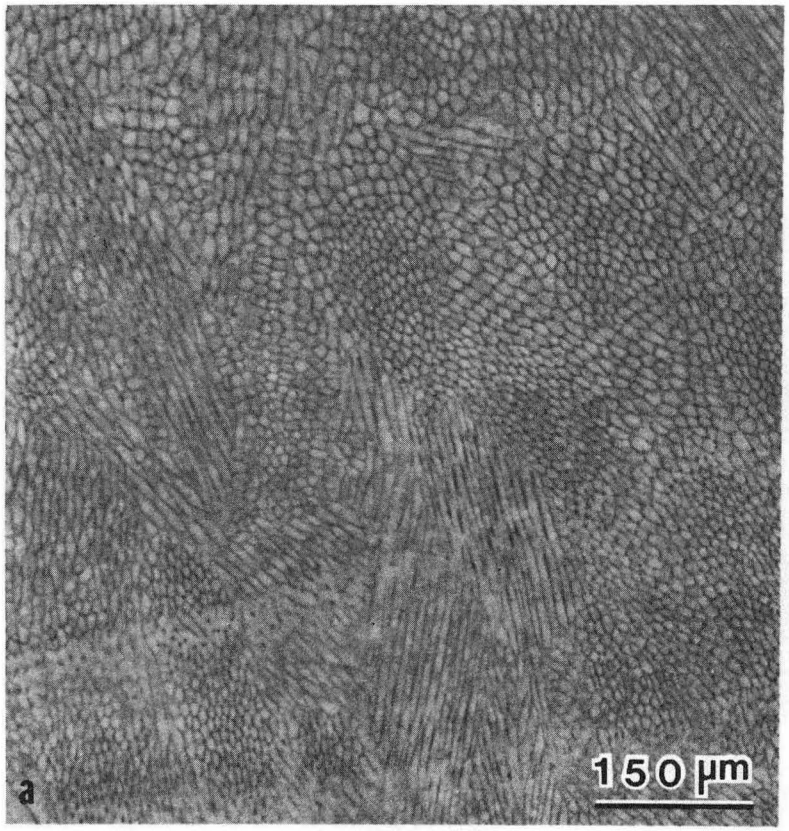

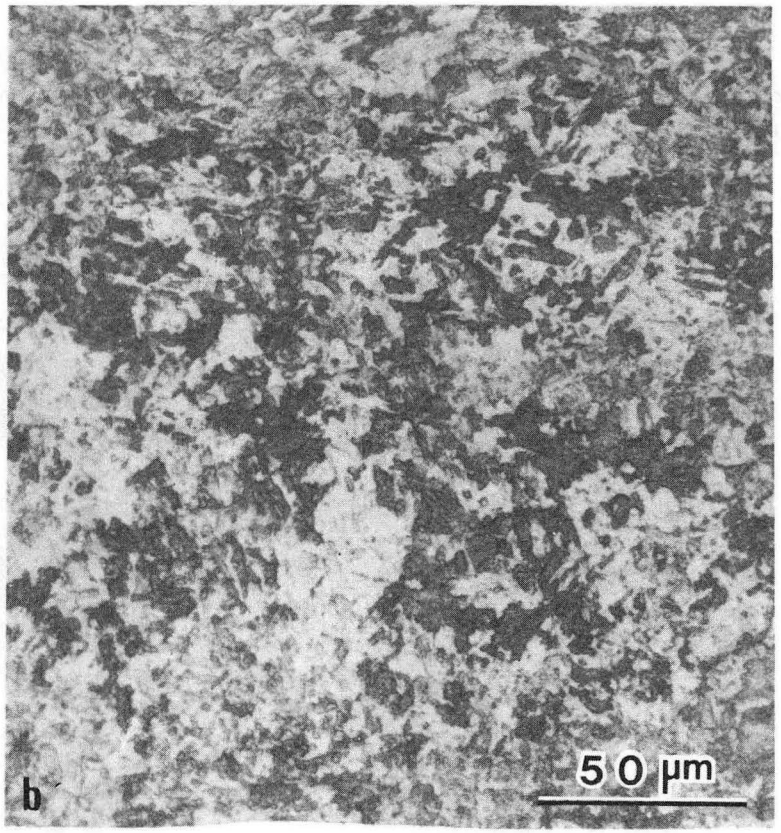

XBB 846-4528

Fig. 7 - Microstructures of all weld deposit specimens etched with (a) 5% Nital and (b) acidified $FeCl_3$ solutions.

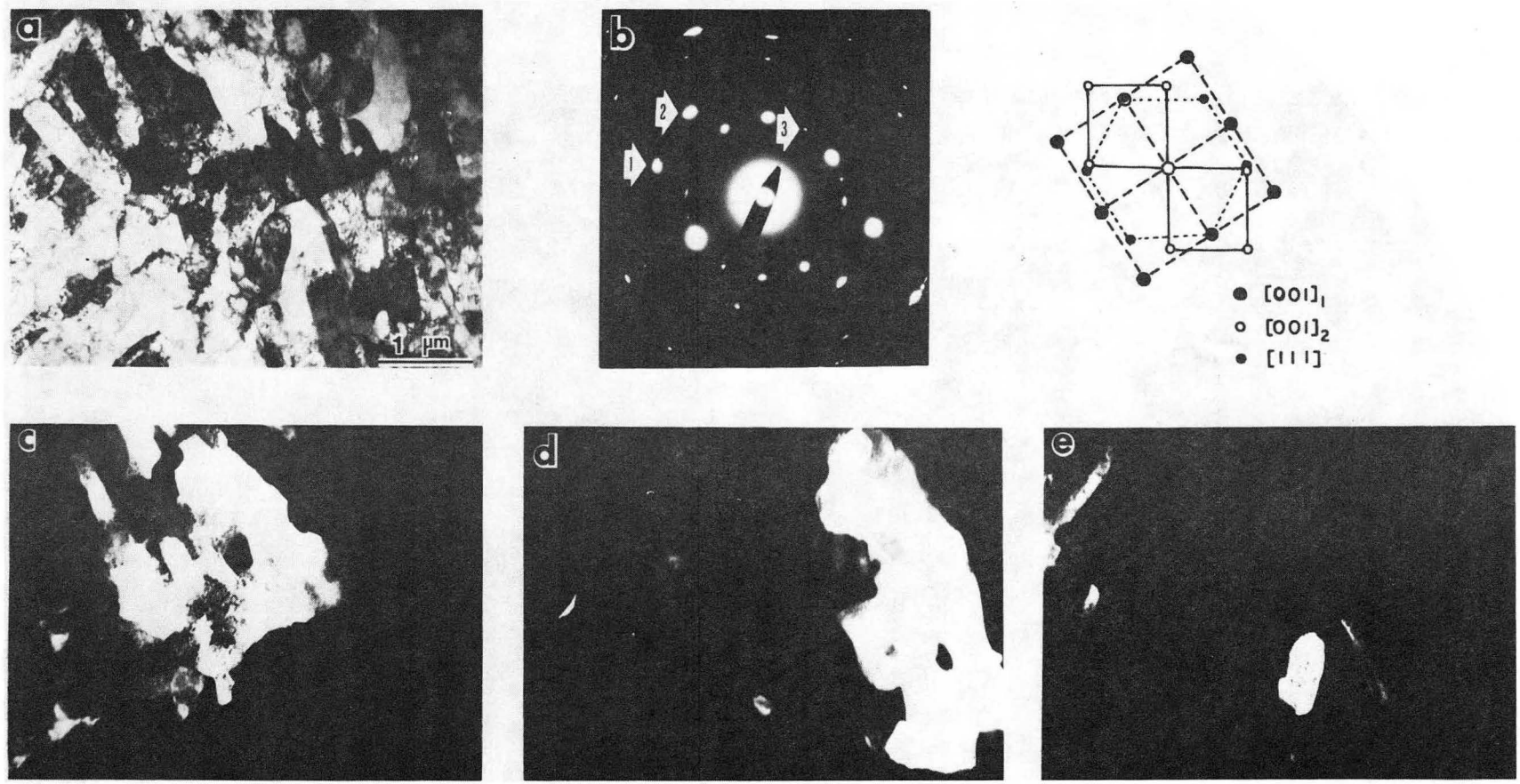

XBB 847-5313

Fig. 8 - Transmission electron micrographs of the multipass weld deposit: (a) bright field image, (b) selected area diffraction pattern, (c), (d) and (e) are dark field images taken from the diffraction spots marked with arrows 1, 2 and 3, respectively in (b).

This report was done with support from the Department of Energy. Any conclusions or opinions expressed in this report represent solely those of the author(s) and not necessarily those of The Regents of the University of California, the Lawrence Berkeley Laboratory or the Department of Energy.

Reference to a company or product name does not imply approval or recommendation of the product by the University of California or the U.S. Department of Energy to the exclusion of others that may be suitable.

LAWRENCE BERKELEY LABORATORY
TECHNICAL INFORMATION DEPARTMENT
UNIVERSITY OF CALIFORNIA
BERKELEY, CALIFORNIA 94720